Molecular Cell
Article

Enhanced Chromatin Dynamics by FACT Promotes Transcriptional Restart after UV-Induced DNA Damage

Christoffel Dinant,[1,2,3] Giannis Ampatziadis-Michailidis,[4] Hannes Lans,[1] Maria Tresini,[1] Anna Lagarou,[4,7] Malgorzata Grosbart,[1] Arjan F. Theil,[1] Wiggert A. van Cappellen,[2] Hiroshi Kimura,[5] Jiri Bartek,[3,6] Maria Fousteri,[4] Adriaan B. Houtsmuller,[2,*] Wim Vermeulen,[1,*] and Jurgen A. Marteijn[1,*]

[1]Department of Genetics, Erasmus Medical Centre, Rotterdam 3015 GE, The Netherlands
[2]Department of Pathology, Erasmus Medical Centre, Optical Imaging Centre (OIC), Rotterdam 3015 GE, The Netherlands
[3]Genome Integrity Unit, Danish Cancer Society Research Centre, Strandboulevarden 49, DK-2100 Copenhagen, Denmark
[4]Institute of Biomedical Sciences, BSRC "Alexander Fleming," 16672 Vari, Athens, Greece
[5]Graduate School of Frontier Biosciences, Osaka University, 565-0871 Osaka, Japan
[6]Institute of Molecular and Translational Medicine, Palacky University, CZ-77515 Olomouc, Czech Republic
[7]Present address: Institut de Pharmacologie et de Biologie Structurale (IPBS), CNRS/UPS, 205 Route de Narbonne, F-31077 Toulouse, France
*Correspondence: a.houtsmuller@erasmusmc.nl (A.B.H.), w.vermeulen@erasmusmc.nl (W.V.), j.marteijn@erasmusmc.nl (J.A.M.)
http://dx.doi.org/10.1016/j.molcel.2013.08.007

SUMMARY

Chromatin remodeling is tightly linked to all DNA-transacting activities. To study chromatin remodeling during DNA repair, we established quantitative fluorescence imaging methods to measure the exchange of histones in chromatin in living cells. We show that particularly H2A and H2B are evicted and replaced at an accelerated pace at sites of UV-induced DNA damage. This accelerated exchange of H2A/H2B is facilitated by SPT16, one of the two subunits of the histone chaperone FACT (facilitates chromatin transcription) but largely independent of its partner SSRP1. Interestingly, SPT16 is targeted to sites of UV light-induced DNA damage-arrested transcription and is required for efficient restart of RNA synthesis upon damage removal. Together, our data uncover an important role for chromatin dynamics at the crossroads of transcription and the UV-induced DNA damage response.

INTRODUCTION

Cells are continuously exposed to endogenous metabolites and environmental agents that induce lesions in DNA. These lesions interfere with transcription and replication, resulting in cellular malfunction and DNA damage-induced mutagenesis of genetic information (Hoeijmakers, 2009). Helix-distorting DNA lesions, for instance, those induced by UV-C exposure, located anywhere in the genome are recognized by the concerted action of XPC- and DDB2-containing complexes to initiate global genome nucleotide excision repair (GG-NER) (Nouspikel, 2009). DNA lesions in the transcribed strand of active genes which interfere with RNA polymerase II (RNApolII) elongation activate a dedicated NER branch, termed transcription-coupled NER (TC-NER) (Hanawalt and Spivak, 2008). Both GG-NER and TC-NER funnel into a shared pathway that removes lesions by helix unwinding, excision of the damaged strand, DNA resynthesis over the single-stranded gap, and nick ligation (Nouspikel, 2009). A complex, as-yet poorly defined mechanism is coupled to TC-NER to allow transcription resumption after completion of TC-NER (Hanawalt and Spivak, 2008).

Transcriptional control is largely dependent on the chromatin structure (Avvakumov et al., 2011). Similarly, efficient DNA repair requires plasticity of the chromatin structure for repair factors to gain access to the DNA template (Soria et al., 2012). Importantly, not only the access of repair factors to the DNA and the subsequent swift repair of DNA lesions is required for the recovery of transcription, but also proper restoration of the predamage chromatin structure (Green and Almouzni, 2003; Smerdon, 1991). Besides posttranslational histone modifications that increase access to DNA, nucleosome sliding and histone removal are thought to expose the DNA and thereby facilitate binding of, for example, DNA repair or transcription factors to damaged DNA (Avvakumov et al., 2011; Gong et al., 2005; Soria et al., 2012). Histone displacement through sliding, removal, and reinsertion into chromatin is achieved by two groups of proteins: ATP-dependent chromatin remodelers and histone chaperones. Remodelers use ATP hydrolysis to remove histones from DNA or slide whole nucleosomes along DNA fibers, a mechanism suggested to promote DNA accessibility (Lans et al., 2012). Histone chaperones primarily load histones onto DNA to restore chromatin after access is no longer required, and conversely they also catalyze histone removal (Avvakumov et al., 2011; De Koning et al., 2007). Accordingly, early steps of NER involve ATP-dependent relaxation of chromatin (Lans et al., 2012; Luijsterburg et al., 2012), whereas restoration of chromatin after NER completion depends on histone chaperones CAF1 and ASF1 (Polo et al., 2006).

Direct measurement of histone removal and reinsertion kinetics in response to DNA damage in living cells, representing

chromatin remodeling in vivo, has escaped scrutiny. We have investigated the dynamics of GFP-tagged histones in living cells in response to UV-C irradiation and discovered an important function for FACT-subunit SPT16 in accelerating the exchange of H2A and H2B and promoting transcription restart after DNA repair of the lesions blocking transcription.

RESULTS

Histone Exchange upon UV-Induced DNA Damage

We designed three methods to determine the mobility of histones after DNA damage induction in living cells. First, we used a fluorescence recovery after photobleaching (FRAP) approach to compare histone mobility in UV-damaged versus unperturbed chromatin in living cells. In cells expressing GFP-tagged histones (Kimura and Cook, 2001), the fluorescence in half of the nucleus was photobleached, and local UV damage (LUD) was introduced in the photobleached part using a UV-C laser (Dinant et al., 2007) (Figure 1A). Incorporation of fluorescent histones in the bleached area will be faster in regions with a higher histone exchange rate, leading to increased local fluorescence. Interestingly, we observed increased fluorescence recovery corresponding to an ~2-fold increased exchange rate of GFP-tagged histones H2A and H2B at the LUD, whereas no accelerated H3.1 or H4 exchange was detected (Figures 1B–1E). Local concentrations of histone proteins were not affected by UV damage (see Figures S1A and S1B online), indicating that the fluorescence increase at LUD after photobleaching directly reflects enhanced H2A/H2B-chromatin exchange rather than histone accumulation. Besides half-nucleus FRAP, we used two alternative approaches to study histone dynamics upon DNA damage. Induction of LUD in cells 6–8 hr after transfection with H2A-GFP, before the incorporation of newly synthesized fluorescent H2A molecules had reached a steady state, resulted in faster increase of fluorescence at damaged areas (Figure S1C). And similarly, upon PEG-mediated cell fusion of cells expressing H2A-GFP with cells expressing H2B-RFP, local UV irradiation caused accelerated incorporation of RFP signals in green nuclei and of GFP signals in red nuclei at LUD (Figure S1D). Both alternative methods confirmed our results obtained by FRAP experiments. DNA damage-induced H2A/H2B exchange was independent of DNA replication, as it occurred in both S phase and non-S phase cells, identified by the presence and absence of characteristic replication foci of mCherry-tagged proliferating cell nuclear antigen (PCNA), which itself is also recruited to LUD both in S phase and non-S phase cells (Essers et al., 2005) (Figure S1E). Together these data clearly show that UV-C irradiation induces accelerated removal from and reincorporation into chromatin of H2A/H2B dimers.

Histone Exchange upon DNA Damage Requires FACT

The key proteins involved in mediating nucleosome assembly are histone chaperones (Ransom et al., 2010). We tested the involvement of two well-studied H2A/H2B chaperones, NAP1L1 (Zlatanova et al., 2007) and FACT (Reinberg and Sims, 2006), in accelerated histone exchange at sites of DNA damage. While siRNA-mediated knockdown of NAP1L1 resulted in a clear reduction of NAP1L1 protein levels, accelerated exchange of H2A at LUD was still observed (Figures S2A and S2B). In contrast, simultaneous siRNA-mediated knockdown of both SSRP1 and SPT16 subunits of the FACT heterodimer resulted in the complete absence of accelerated H2A exchange at LUD, compared to control transfected cells (Figure 2A, Figures S2C and S2D). Importantly, only a small decrease of general H2A exchange was observed in unperturbed regions upon FACT depletion (Figure S2D).

It has been described that FACT is modified by posttranslational modifications upon DNA damage, thereby regulating its interaction with chromatin. SSRP1 becomes phosphorylated by CK2 upon UV damage (Krohn et al., 2003), while the SPT16 subunit gets PARylated by PARP1 upon oxidative damage (Heo et al., 2008; Huang et al., 2006). To test whether these FACT modifications are involved in UV-induced accelerated histone exchange, we performed the live-cell histone exchange assay in the presence of PARP1 or CK2 inhibitors. No effect on the H2A exchange was observed upon CK2 inhibition (Pagano et al., 2004), while a small decrease in H2A exchange was found when PARP1 was inhibited (Menear et al., 2008) (Figures S2E–S2H), indicating that PARylation events, possibly of SPT16 itself, have a minor stimulatory effect on histone mobility upon UV damage.

The Role of SPT16 in the DNA Damage Response

To investigate in more detail the in vivo role of FACT during the UV-induced DNA damage response (UV-DDR), we generated stable cell lines expressing full-length GFP-tagged SSRP1 or SPT16 (Figure S3A). Both SSRP1 and SPT16 accumulated at sites of LUD in living cells (Figure 2B). In addition, antibody staining of endogenous SPT16 confirmed colocalization both with CPD (cyclobutane pyrimidine dimer), a marker for UV damage, and with sites of increased H2A-GFP exchange (Figure 2C). This recruitment to sites of DNA damage is a reversible event, as it was no longer detected 24 hr after DNA damage infliction, when most lesions are removed (Figure S3B).

NER is the main DNA repair system that removes helix-distorting lesions such as CPDs induced by UV-C irradiation. We used the ChIP-on-western technique, a dedicated chromatin immunoprecipitation (ChIP) procedure based on classical ChIP, and optimized to reveal the composition of transient protein complexes at damaged DNA (Coin et al., 2008; Fousteri et al., 2006; Kannouche et al., 2004) to study the in vivo composition of FACT-associated complexes upon UV damage induction. This approach showed that SPT16 coimmunoprecipitated with the core NER factor XPB (p89 subunit of TFIIH) upon UV irradiation. Another core NER factor, XPA, used as positive control, also coprecipitated with p89 (Figure 2D). These data indicate the presence of SPT16 at chromatin sites undergoing NER. RNAi-mediated knockdown of both FACT subunits in NER-proficient HeLa cells led to increased sensitivity to UV-C irradiation (Figure 2E), indicative of a function in the UV-induced DDR. Strikingly, while expression of both FACT subunits was efficiently reduced (Figure S2C), knockdown of the SSRP1 subunit alone did not result in UV sensitivity, whereas depletion of only SPT16 resulted in similar UV hypersensitivity to simultaneous knockdown of both FACT subunits. Consistent with the effect on UV survival, knockdown of SPT16 strongly reduced the H2A exchange upon UV damage, while SSRP1 depletion did not have a clear effect on histone exchange (Figure S3C). These data suggest that the

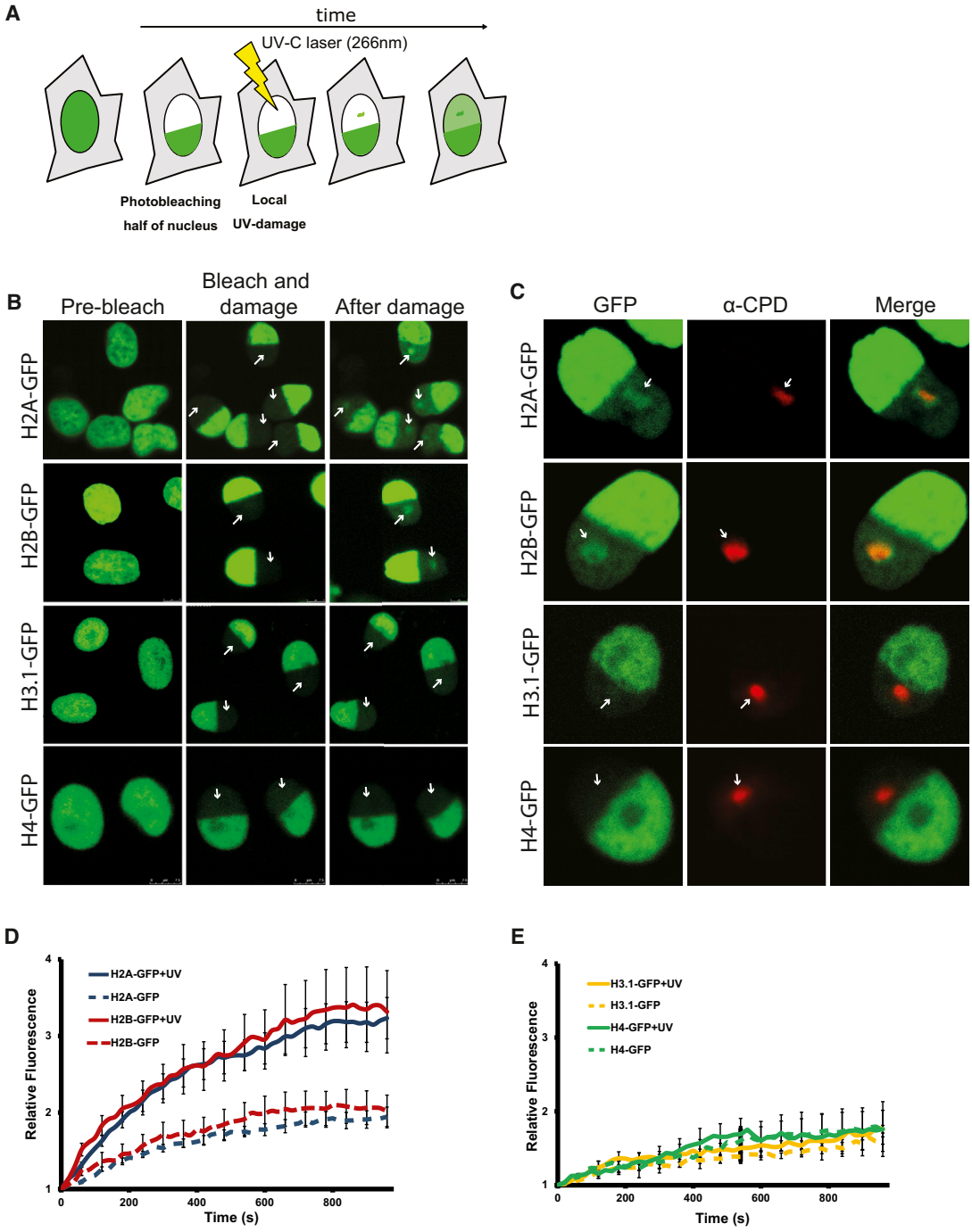

Figure 1. Increased Histone H2A and H2B Exchange at UV-Induced DNA Damage

(A) Method for measuring histone exchange at local laser-directed UV-C DNA damage (LUD). Half of the nucleus of cells stably expressing GFP-tagged histones is photobleached. In the photobleached part, UV-C damage is inflicted with a UV-C (266 nm) laser. Recovery of fluorescence for both damaged and undamaged areas is measured.

(B) H2A-GFP and H2B-GFP exchange is accelerated at LUD, whereas H3.1-GFP and H4-GFP do not display DNA damage-induced accelerated exchange rates. (Left panel) Unbleached cells, (middle panel) images of half nucleus bleached immediately captured after local UV-C damage infliction, and (right panel) 15 min after UV damage.

(C) Accelerated histone exchange localizes to damaged areas marked by CPD staining. (Left panel) GFP signal, (middle panel) anti-CPD (cyclobutane pyrimidine dimer) antibody staining used as UV-induced DNA damage marker, and (right panel) merge of GFP and anti-CPD signals.

(D and E) Quantification of histone exchange in unperturbed or locally UV-C-exposed regions of the bleached part of the nucleus. Fluorescence recovery directly after LUD is plotted against time in seconds for H2A– and H2B-GFP (D) and H3.1- and H4-GFP (E) (n > 12 cells, mean ± SEM). See also Figure S1.

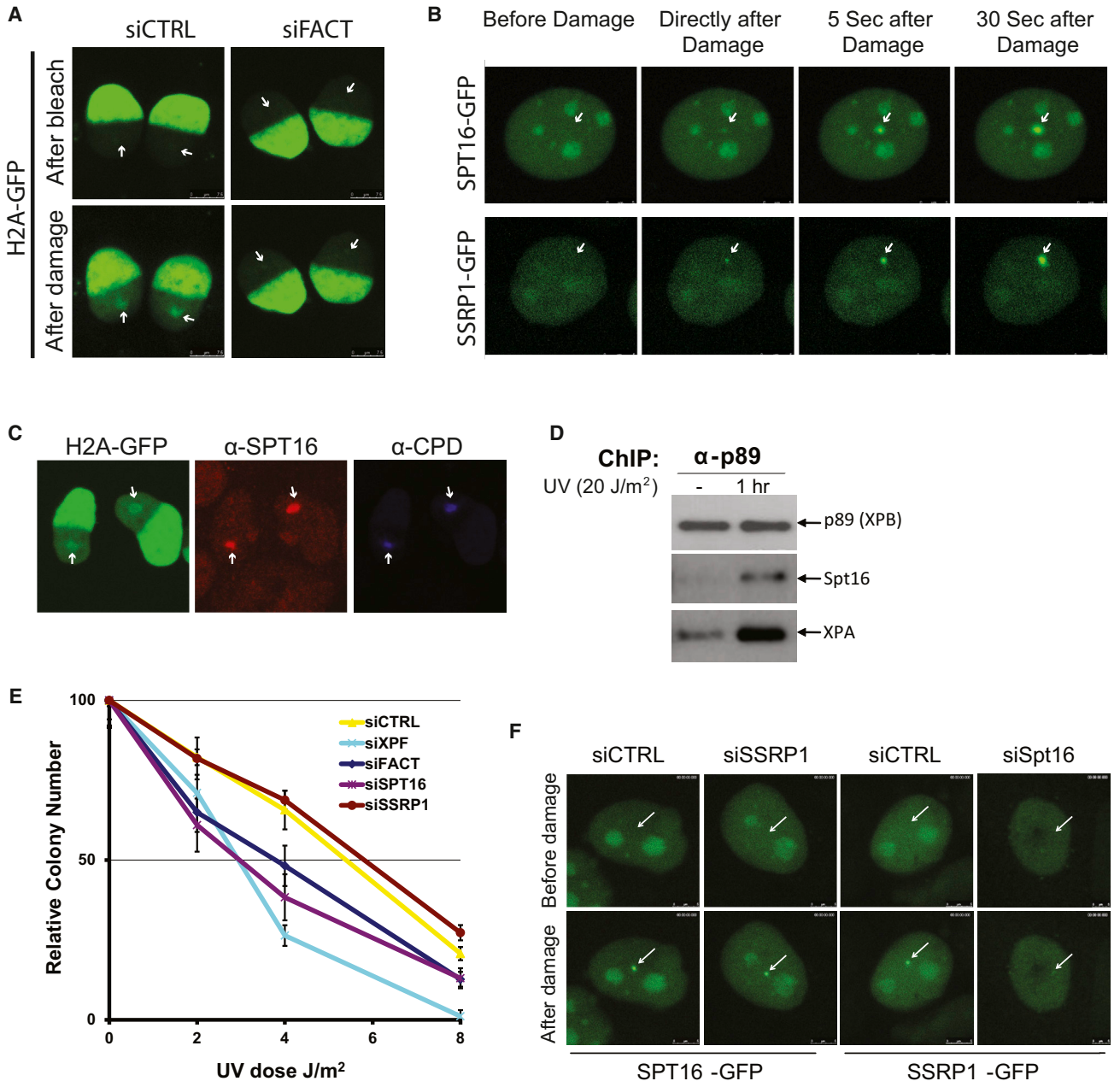

Figure 2. H2A Exchange Is Dependent on the SPT16 Subunit of FACT

(A) H2A-GFP histone exchange after siRNA transfection of nontargeting control or siRNA targeting both SSRP1 and SPT16 together (siFACT). (Top row) Immediate after LUD induction, (bottom row) 30 min after LUD.

(B) Live-cell imaging analysis after LUD infliction (arrow) in MRC5 cells stably expressing SPT16-GFP (top row) and SSRP1-GFP (bottom row).

(C) Immunofluorescent analysis of SP16 accumulation on LUD. GFP-H2A-expressing cells with a bleached half nucleus were fixed 30 min after LUD infliction, GFP imaged (left panel), and immunostained for SPT16 (middle panel) and CPD (right panel). SPT16 accumulates at LUD and colocalizes with accelerated exchange of H2A-GFP and CPD staining.

(D) ChIP-on-western analysis of mock and UV irradiated (1 hr after 20 J/m^2) in vivo crosslinked VH10 (sv40) cells chromatin immunoprecipitated with p89 antibodies. Samples were normalized to p89 levels; immunoblot analysis of the coimmunoprecipitated proteins was performed for SPT16 and XPA.

(E) UV-C sensitivity of HeLa cells with siRNA-mediated knockdown for the indicated proteins, determined by colony-forming ability (mean ± SD).

(F) SPT16-GFP is recruited to LUD in cells treated with control or SSRP1 siRNA, but SSRP1-GFP does not accumulate at LUD in the presence of siRNA against SPT16. See also Figure S2.

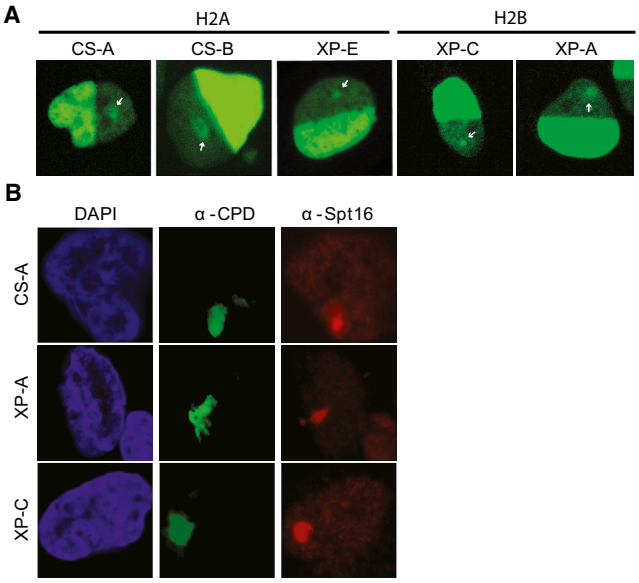

Figure 3. NER-Independent FACT Implication in UV-DDR

(A) Accelerated histone exchange in CS-A, CS-B, and XP-E patient cells expressing H2A-GFP; XP-C patient cells expressing H2B-GFP; and XP-A patient cells expressing H2B-YFP. Arrow indicates site of LUD.

(B) Endogenous SPT16 localizes to LUD as indicated by staining with anti-CPD antibodiesin CS-A, XP-A, and XP-C cells. See also Figure S3.

SPT16 function at damaged chromatin does not require SSRP1. In addition, accumulation of SSRP1-GFP at LUD required SPT16 expression, whereas SPT16 was recruited to LUD in the absence of SSRP1 (Figure 2F and Figure S3E). Together these results indicate that although SSRP1 is present at sites of DNA damage, only its partner in the FACT heterodimer, SPT16, plays an important role in the UV-DDR.

Accelerated Histone Exchange Occurs Also in the Absence of NER

NER is initiated by two damage recognition pathways. When lesions are present specifically in the transcribed strand of active genes and block RNApolII-mediated transcription elongation, they are targeted by TC-NER, whereas lesions located anywhere in the genome can trigger GG-NER (Nouspikel, 2009). Interestingly, neither accumulation of SPT16 at LUD nor the accelerated exchange of H2A/H2B required initiation of NER. Both still occurred in the absence of damage recognition factors for GG-NER (in patient cells lacking functional XPC or DDB2) or for TC-NER (in patient cells lacking functional CSA or CSB) (Figures 3A and 3B). Also in cells derived from an XP-A patient, in which both NER subpathways are defective due to the complete absence of the crucial NER factor XPA, H2A exchange and SPT16 accumulation still took place (Figures 3A and 3B). These data suggest that both targeting of Spt16 and damage-induced accelerated histone exchange occur independent of NER.

SPT16 Is Involved in Transcription Restart after TC-NER Completion

Because SPT16 is involved in the survival upon UV-C induced damage (Figure 2E), we determined whether SPT16 activity specifically affects TC-NER or GG-NER. RNAi-mediated knockdown of both FACT subunits did not interfere with the recruitment of early GG-NER factors XPC and DDB2, nor with TC-NER factor CSB (Figure S4A), suggesting that the role of SPT16 in the UV damage response is not needed for the recruitment of these factors that are involved in damage recognition. A ChIP-on-western analysis after immunoprecipitation with an antibody against DDB1, which functions in both GG-NER and TC-NER via interactions with DDB2 and CSA, respectively (Fousteri et al., 2006; Groisman et al., 2003), revealed a clear enrichment of endogenous SPT16 and SSRP1 in active chromatin-bound NER complexes in NER-proficient cells upon UV-C damage induction (Figure 4A). However, in CS-B patient cells (GG-NER proficient), where DDB1 can only be recruited to DNA damage via the GG-NER factor DDB2 (Fousteri et al., 2006), SPT16 did not coimmunoprecipitate with DDB1, indicating that SPT16 specifically binds to chromatin sites undergoing TC-NER and not GG-NER. In line with this, ChIP-on-western for SPT16 revealed that in the absence of CSB, when no functional TC-NER complexes are formed (Fousteri et al., 2006), no UV-induced interaction with XPA was observed (Figure S4B). The specific presence of SPT16 in TC-NER complexes was further confirmed by ChIP-on-western experiments with the elongating form of RNApolII (RNApolIIo) and the TC-NER master organizer CSB (Figure 4B). Moreover, ChIP for p89 (XPB) showed an interaction with the FACT complex in XP-C patient cells (TC-NER proficient), but not in CS-B patient cells, indicating that FACT can only be found in the vicinity of active NER proteins at UV-damage-blocked transcription sites and not at UV lesions in the rest of the genome (Figure S4C). It is important to mention that the CSB-dependent interaction in these ChIP experiments only indicates that SPT16 specifically interacts with the TC-NER complex. It does not show that CSB is required for the SPT16 recruitment to DNA damage. On the contrary, the FACT-facilitated H2A/H2B exchange at the site of damage occurred independently of CS proteins (Figures 3A and 3B). Accordingly, in the absence of CSB, SPT16 coimmunoprecipitated with RNAPolIIo (Figure S4D), whereas binding of most of the other TC-NER-specific factors is dependent on the presence of CSB (Fousteri et al., 2006; Schwertman et al., 2012). Together these results show that while FACT is present at sites of active TC-NER, the recruitment to this repair complex is mediated via a different mechanism.

A key event in the initiation of TC-NER is the stalling of RNApolII on DNA lesions, which results in the stable association of the TC-NER-specific factors CSA and CSB (Fousteri et al., 2006). We tested whether stalling of RNApolII at DNA lesions itself might be the trigger to recruit FACT as well, thereby initiating the H2A/H2B histone exchange at sites of UV damage. Inhibition of active transcription by RNAPolII using DRB or α-amanitin (Bensaude, 2011), which effectively blocks the accumulation of TC-NER proteins (Schwertman et al., 2012; van den Boom et al., 2004), did not interfere with H2A-GFP exchange at LUD or SPT16 accumulation (Figures 4C and 4D and Figure S4E). In addition, FRAP experiments showed no difference in mobility of SPT16 upon RNApolII transcription inhibition, indicating that stalling of RNApolII, in the absence of UV-C damage, is not sufficient to immobilize SPT16 (Figures S4F and S4G). Together this

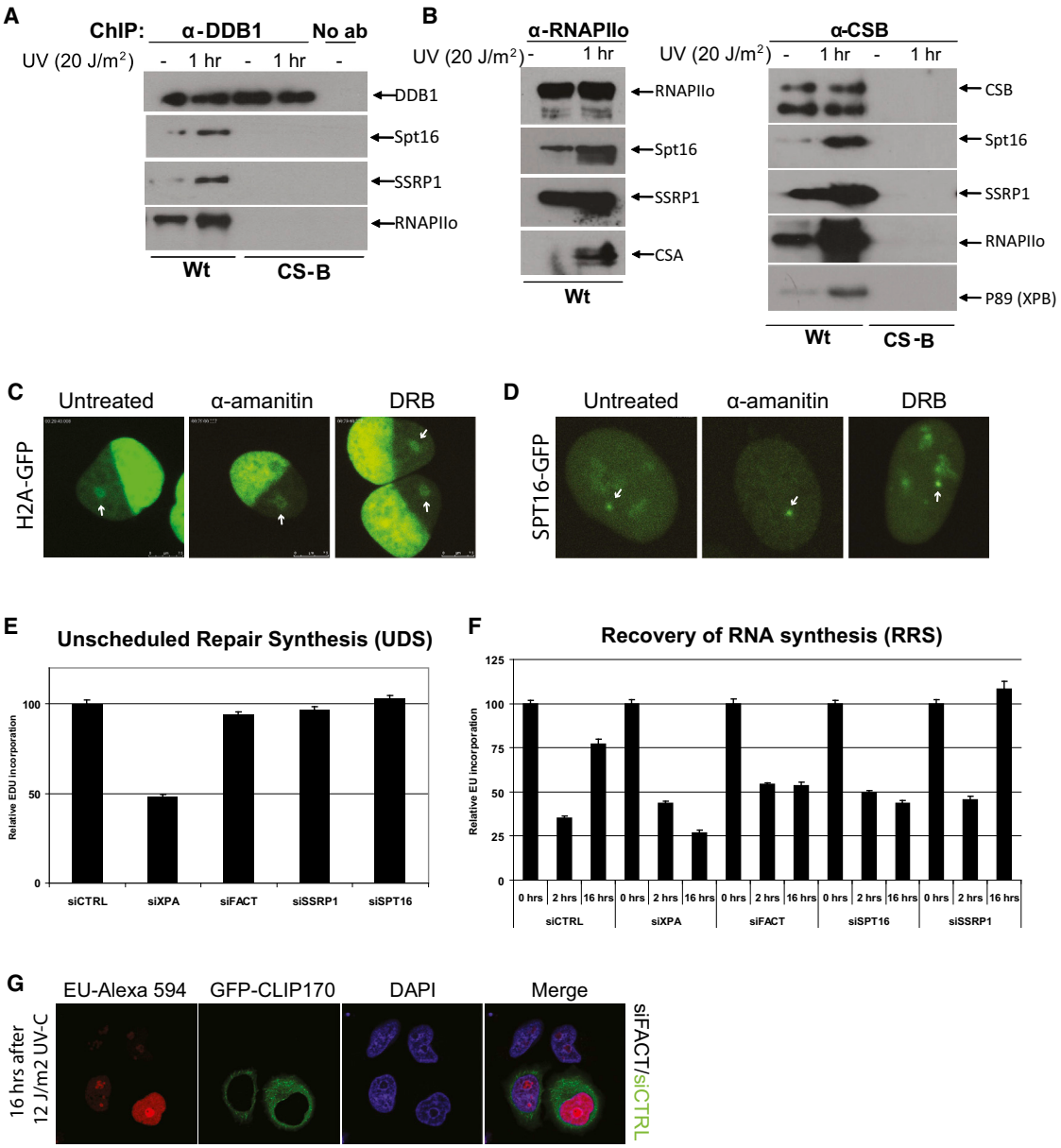

Figure 4. SPT16 Is Specifically Involved in TC-NER

(A) Mock and UV irradiated (1 hr after 20 J/m^2) VH10 and CS1AN (CS-B) cells were in vivo crosslinked and chromatin immunoprecipitated with DDB1 antibodies for ChIP-on-western analysis. RNApolIIo (elongating form) and both FACT subunits only coimmunoprecipitated with DDB1 in TC-NER-proficient cells, indicative for their TC-NER-specific role.

(B) RNApolIIo and CSB ChIP with and without UV irradiation (1 hr after 20 J/m^2) in hTert-immortalized VH10 cells and CS1AN (CS-B) cells, showing UV-induced association of FACT to TC-NER complexes. CSB ChIP in CS-B cells is shown as a control for antibody specificity. For (A) and (B), samples were normalized to equal levels of the chromatin immunoprecipitated protein. Immunoblot analysis of the coimmunoprecipitated proteins was performed with antibodies as indicated.

(C and D) (C) Accelerated exchange of H2A-GFP or (D) recruitment of SPT16-GFP was not affected by transcription inhibition by 16 hr of α-amanitin (25 μg/ml) or 2 hr of DRB (100 μM) before damage infliction.

(E) Unscheduled DNA repair synthesis (UDS) determined by EdU incorporation over 3 hr immediately after UV-C exposure (16 J/m^2) in hTert-immortalized C5RO cells after siRNA-mediated knockdown of the indicated proteins. (n > 200 cells per sample; RFI, relative fluorescence intensity; mean ± SEM).

(F) Recovery of RNA synthesis (RRS) after UV-induced inhibition, using 2 hr pulse labeling with EU without UV damage and 2 and 16 hr after UV-C exposure (8 J/m^2) in U2OS cells after siRNA-mediated knockdown of the indicated proteins. Values were normalized to predamage values (n > 200 cells per sample; RFI, relative fluorescence intensity; mean ± SEM).

(G) U2OS cells expressing GFP-CLIP170 (Dragestein et al., 2008) (for identification of siCTRL-transfected cells) were transfected with siCTRL and mixed with cells cotransfected with siSSRP1 and siSPT16. Transcription levels 16 hr after 12 J/m^2 as determined by 2 hr pulse labeling with EU were not recovered in SRRP1/Spt16 knockdown cells. After fixation, EU is fluorescent labeled with Alexa 594. See also Figure S4.

shows that histone exchange facilitated by FACT at sites of UV-C damage-stalled transcription is not dependent on RNApolII stalling, nor does it require the presence of NER factors. This indicates that FACT recruitment to DNA damage is either a very early step in the NER pathway or occurs in parallel to, and independently of, NER.

We found that RNAi-mediated knockdown of SPT16 had no effect on the amount of unscheduled DNA synthesis (UDS) after UV-C damage, which is a measure for GG-NER activity (Stefanini et al., 1993) (Figure 4E). Together with the absence of FACT near DNA lesions recognized by GG-NER (Figure 4A, Figure S4C), these data confirm that SPT16 has no essential function in GG-NER. Stalling of RNApolII at UV lesions causes inhibition of RNA synthesis. In TC-NER-proficient cells, recovery of RNA synthesis (RRS) after UV-induced inhibition usually starts several hours after damage infliction, when transcription-blocking lesions have been removed (Mayne and Lehmann, 1982). Interestingly, similar to depletion of the essential NER gene *XPA*, knockdown of both FACT subunits or of SPT16 alone resulted in a strong decrease in RRS (Figures 4F and 4G). Together these data indicate that, by promoting accelerated histone exchange, SPT16 plays an important role in the completion of TC-NER, allowing efficient restart of transcription after repair of the blocking lesions.

DISCUSSION

Here, we provide evidence for a role of the histone chaperone FACT in promoting transcription resumption after DNA damage-induced inhibition. FACT aids passage of RNApolII through chromatin templates by destabilizing the nucleosomes through the exchange of a histone H2A/H2B dimer (Hsieh et al., 2013; Reinberg and Sims, 2006). In addition, FACT is known to deposit the H2A/H2B dimer immediately behind the elongating transcription complex, likely to restore a more closed chromatin structure, thereby repressing intragenic transcription initiation from cryptic sites (Carvalho et al., 2013; Reinberg and Sims, 2006). The combined action of both removal and deposition of H2A/H2B during and immediately following transcription, respectively, also explains the observed transcription-dependent increased exchange of these dimers (Kimura and Cook, 2001). The ability of FACT to remove and reinsert H2A/H2B histones into chromatin in vitro has implicated it in all major DNA-associated processes, i.e., replication, transcription, and repair (Heo et al., 2008; Reinberg and Sims, 2006; Winkler and Luger, 2011). In addition, FACT has been shown to act during the UV-induced DDR in association with Casein Kinase II (CK2), in a role unrelated to chromatin remodeling (Keller and Lu, 2002; Krohn et al., 2003).

We found that the SPT16-dependent accelerated H2A/H2B exchange occurs specifically at sites of damage-arrested transcription and is important for efficient recovery of UV-inhibited RNA synthesis. Surprisingly, lesion recognition by stalled RNApolII is not required for SPT16 recruitment or accelerated H2A/H2B exchange at damaged sites, suggesting that this action occurs prior to or in parallel to TC-NER activation. Interestingly, these data show that the SPT16 histone chaperone activity is recruited independently from the ATP-dependent chromatin remodeler CSB (Citterio et al., 2000; Lans et al., 2012); however, both chromatin-remodeling activities are needed for efficient transcription-coupled repair. Importantly, the fact that H2A/H2B exchange still takes places at damaged chromatin in the absence of functional TC-NER and that recruitment of TC-NER factors occurs in the absence of FACT or enhanced H2A/H2B exchange shows that this exchange is not required to trigger TC-NER, nor is it a consequence of DNA repair itself.

The FACT heterodimer can be posttranslationally modified by phosphorylation of SSRP1 by CK2 and by PARylation of SPT16 by PARP1 (Huang et al., 2006; Krohn et al., 2003). In our assay, CK2 inhibition had no effect on FACT activity, but PARP inhibition slightly decreased histone exchange at UV damage. This suggests that FACT recruitment or activity is stimulated by PARylation, a finding that conflicts with earlier studies showing that PARP1 activity inhibits FACT-directed H2AX exchange and promotes FACT dissociation from chromatin in vitro (Heo et al., 2008; Huang et al., 2006). This discrepancy might be explained by assuming that PARylation of factors that were not present in these in vitro experiments contributes to nucleosome plasticity in living cells. More experiments are needed to determine the precise role of PARP1 with regards to histone exchange in response to DNA damage.

We have shown that H2A/H2B exchange is essential to promote transcription restart by RNApolII. There are multiple points during TC-NER where FACT activity might be required. Figure 5 describes three possible scenarios for FACT functions at sites of UV-damage-induced stalled transcription. In scenario 1, nucleosome deassembly behind the transcribing RNApolII is required for lesion-blocked RNApolII to reverse translocate (backtrack) (Cheung and Cramer, 2011). As removal of the blocking lesion is shown to occur via a nonallosteric recruitment of repair factors in the presence of RNAPII (Brueckner et al., 2007), remodeling of the chromatin in the vicinity of lesion-stalled RNAPolII is necessary to provide access of repair factors to the otherwise hidden blocking lesion. In this situation, the action of SPT16 will provide sufficient chromatin plasticity to remodel the arrested transcription complex to ensure efficient recruitment and activity of TC-NER proteins. Increased histone turnover might also promote the recruitment of a thus-far-unknown protein that is required for efficient repair and/or transcription restart after repair (scenario 2, Figure 5). The recruitment of such a protein could also occur via a direct interaction with SPT16, rather than indirectly through histone exchange. In scenario 3, accelerated exchange of H2A and H2B is required specifically for the restart of the stalled polymerase, or even damage bypass (Walmacq et al., 2012). In both situations prolonged enhanced plasticity of chromatin would allow a repeated cycle of failed transcription reinitiation events to take place, until a successful attempt leads to normal levels of histone exchange again. These three scenarios are by no means mutually exclusive and may even take place in a specific temporal order. These scenarios are likely not restricted to blocked transcription at NER-initiating lesions but may occur at any other type of damage that interferes with RNA polymerase elongation, such as collisions between RNA and DNA polymerases (Bermejo et al., 2012) or other lesions.

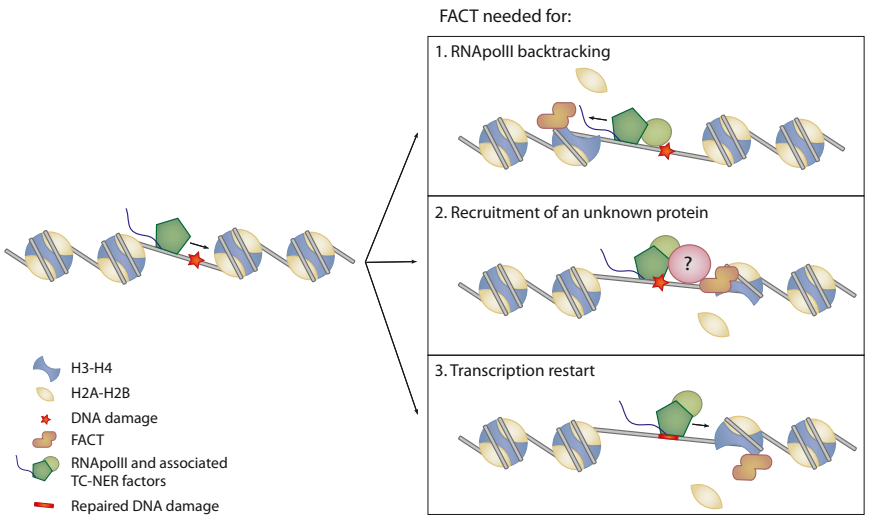

Figure 5. Three Scenarios for the Function of FACT-Induced Accelerated Histone Exchange at UV-Induced DNA Damage

Upon stalling of RNAPolII on a UV lesion, the following three events may take place. In scenario 1, removal of an H2A-H2B dimer provides space for RNApolII to reverse translocate, which in turn allows efficient recruitment of downstream TC-NER proteins. In scenario 2, an unidentified TC-NER protein needs to be recruited to the DNA damage. This recruitment can only take place when H2A and H2B are removed via FACT, or via a direct interaction with FACT that is present near the damage site. In scenario 3, restart of transcription after TC-NER completion requires elevated levels of histone exchange mediated by FACT.

The finding that specifically the SPT16 subunit of FACT seems required, rather than the complete heterodimeric complex, suggests a damage-specific chromatin-remodeling activity separating it from the canonical FACT function in transcription regulation in which both subunits are involved. It should be noted that, as is often the case for heterodimeric protein complexes, siRNA-mediated knockdown of SSRP1 also results in the reduction of SPT16 protein levels, but not to the same extent as SPT16 knockdown itself (Figure S2C). The remaining SPT16 protein levels upon SSRP1 siRNA depletion are apparently sufficient to perform its function in the UV-DDR. The separation of function between the SPT16 and SSRP1 subunits was unexpected because SSRP1 has been shown to bind to both cisplatin- and UV-C-induced DNA lesions via its HMG1 domain (Krohn et al., 2003; Yarnell et al., 2001). There are only limited additional data available for a separation of function between SPT16 and SSRP1. Thus far only SSRP1 has been found to have an independent-of-SPT16 role in the transcription of a small subset of genes (Li et al., 2007). In spite of that, deletion of the SSRP1 homolog Pob3 in *S. pombe* is viable, but deletion of Spt16 is not (Lejeune et al., 2007). Other studies showing a function for only SSRP1 or SPT16 did not directly compare the activities of both FACT subunits. Recent mechanistic studies on FACT revealed that a C-terminal domain on SPT16, SPT16M, is mainly responsible for the interaction with nucleosomes and can bind to multiple sites on both H3-H4 and H2A-H2B histones, thereby shielding H2A-H2B from interactions with DNA, making space for the HMG1 domain of SSRP1 to bind DNA (Hondele et al., 2013; Kemble et al., 2013; Winkler et al., 2011). Other domains on SPT16 and SSRP1 bind nucleosomes cooperatively with SPT16M (Stuwe et al., 2008; Winkler et al., 2011). This suggests that FACT recruitment to nucleosomes is initiated by SPT16 and is in line with our observations that SSRP1 recruitment to DNA damage is dependent on SPT16. The recruitment of SPT16 to chromatin occurs partly via histone tail interactions (Winkler et al., 2011), which in turn suggests that SPT16 might be targeted to damaged chromatin via a histone tail modification that may occur quickly in response to UV-C irradiation.

The method we have developed and applied here allows direct determination of in vivo histone dynamics at subnuclear regions in living cells. Using this technique we have uncovered a link between UV damage-induced chromatin remodeling and the restart of RNA synthesis. The regulation of the resumption of transcription after repair is highly important, given that improper restart leads to cellular malfunction and apoptosis, and that DNA damage-induced derailment of transcription is an important contributor to aging (Hanawalt and Spivak, 2008; Hoeijmakers, 2009).

EXPERIMENTAL PROCEDURES

Cell Lines and Constructs

HeLa, U2OS, MRC5, XP4PA (XP-C), XP4PA (+GFP-XPC), CS3BE (CS-A), CS1AN (CS-B), CS1AN (+GFP-CSB), and VH10 (DDB2-GFP) (both sv40 and hTert immortalized) cells were cultured under standard conditions in DMEM/F10 medium supplemented with 10% fetal calf serum and antibiotics at 37°C and 5% CO_2. The H2B-GFP-, H3.1-GFP-, and H4-GFP-expressing cells have been previously published (Kimura and Cook, 2001). GFP-H2A (kind gift from Dr. M. Luijsterburg) and H2B-RFP were stably expressed in HeLa cells using neomycin selection. U2OS expressing GFP-tagged SPT16 and SSRP1 were, respectively, hygromycin and neomycin selected. The observed nuclear localization with enriched signal in nucleoli (Birch et al., 2009) is indicative of proper biological activity of these tagged proteins. For cell fusion experiments, cells were fused with 50% polyethylenegycol 1500 in PBS for 1.5 min as described in Schmidt-Zachmann et al. (1993). DNA constructs were transfected with FuGENE HD (Roche Applied Science), and siRNA transfections were performed using RNAiMax (Invitrogen) or Hiperfect (QIAGEN) according to the manufacturer's instructions. Small interfering RNAs (smartpool) against SSRP1, SPT16, and NAP1L1 were supplied by Dharmacon. PARP1 inhibitor (AZD2281) and CK2 inhibitor (2-dimethylamino-4,5,6,7-tetrabromo-1H-benzimidazole [DMAT]) were used 1 hr before damage infliction at a final concentration of 10 μM. Transcription was inhibited with α-amanitin (25 μg/ml) or DRB (100 μM) for the indicated times.

Microscopy

For local UV-C irradiation experiments, a 2 mW pulsed (7.8 kHz) diode-pumped solid-state laser emitting at 266 nm (Rapp OptoElectronic, Hamburg GmbH) was connected to a Zeiss LSM 510 confocal microscope with an axiovert 200 M housing adapted for UV by all-quartz optics or to a Leica SP5 confocal microscope as described (Dinant et al., 2007; Schwertman et al.,

2012). By focusing the UV–C laser inside cell nuclei without scanning, only a limited area within the nucleus (diffraction limited spot) was irradiated. Cells for these experiments cells were grown on 25 or 24 mm diameter quartz coverslips to allow deep UV light to pass through the coverslip. Cells were imaged and irradiated through a 100× 1.2 NA Ultrafluar quartz objective. Immunofluorescence experiments were executed as described (Marteijn et al., 2009). FRAP experiments were performed as described previously (Hoogstraten et al., 2002). All FRAP data were normalized to the average prebleached fluorescence after removal of the background signal. All FRAP curves represent an average of at least 12 measured cells.

Plasmid Constructs

Murine pCMV-Myc-SSRP1 and pCMV4a-SPT16 were a kind gift of Professor Masayuki (Kihara et al., 2008). SSRP1 was amplified by PCR; during this reaction, SalI and XhoI were added to the cDNA and cloned in PCR2.1 (Invitrogen). From this vector, SSRP1 was cloned into peGFP-N1 using Sal1/Xho1. To generate SPT16:GFP:HA the open reading frame (minus the STOP codon) of SPT16 was PCR amplified using primers that contained restriction sites for Hind III (forward) and BamHI (reverse). The amplified fragment was subcloned in a pLHCX retroviral expression vector (Clontech Laboratories) which was previously modified to contain, following a BamHI restriction site, eGFP (minus the initiation and stop codons), followed by the hemagglutinin (HA) tag and a STOP codon. PCR amplifications were performed on a MJ Scientific, Inc., PTC-100 Thermocycler using Phusion polymerase (Bioke). Amplified DNAs were purified using the Promega Wizard PCR purification kit. Following restriction digestion of the inserts and vectors, shrimp alkaline phosphatase treatment of the vectors, and agarose gel electrophoresis, the gel-excised DNAs were purified using the Promega Wizard gel extraction kit. DNA concentrations were calculated by spectrophotometry, and inserts were ligated into vectors at a 3:1 molar ratio. Plasmid DNAs were analyzed by restriction digestion and sequencing.

Antibodies

For ChIP rabbit polyclonal RNApolII (Abcam), α-p89/XPB (S-19, Santa Cruz), α-DDB1 (Abcam), α-Spt16 (clone H-300), and α-ERCC6 antibodies (Santa Cruz) were used. For western blot, α-RNApolII (H5, Babco; and Ser2, Active Motif), α-XPA (Abcam), α-GFP (Roche and Santa Cruz), α-CSB (E-18, Santa-Cruz), α-CSA, α-p89/XPB (S-19, Santa Cruz), α-SSRP1 (clone 10D7, Abcam and clone D-7 Santa Cruz), and α-Spt16 (clone H-300, Santa Cruz) were used. Odyssey compatible secondary antibodies were from LI-COR, and horseradish peroxidase (HRP)-conjugated secondary antibodies were from Dako (α-mouse and α-goat), Southern Biotech (α-rabbit), and Sigma (α-IgM). For immunofluorescence, the following antibodies were used: α-NPM/B23 (Abcam), α-PAR (Alexis, Clone H10), α-Spt16 (clone H-300, Santa Cruz), and α-CPD (TDM-2, MBL International) in combination with the corresponding secondary antibodies labeled with Alexa Fluor 488 or 594 as indicated (Invitrogen; The Jackson Laboratory). Immunofluorescence experiments were executed as described (Marteijn et al., 2009).

Clonogenic Survival Assay

Cells from indicated cell lines seeded in triplicate in 6-well plates (300 cells/well) were treated with UV-C 1 day after seeding and recovered for 1 week before colonies were fixed and stained in 50% methanol, 7% acetic acid, and 0.1% Coomassie blue.

Recovery of RNA Synthesis and Unscheduled DNA Synthesis after UV Irradiation

Fluorescence-based RRS and UDS were performed as described (Nakazawa et al., 2010; Schwertman et al., 2012). In short, for RRS, the indicated cell lines were UV rradiated with 12 J/m^2. Transcription levels were determined 16 hr after UV by 2 hr ethynyluridine (EU)-incorporation. For UDS, VH10 cells were UV irradiated with 16 J/m^2 48 hr after siRNA, and UDS was determined after 3 hr of 5-ethynyl-2′-deoxyuridine (EdU) incorporation. RRS and UDS were quantified by determining fluorescent intensities of >200 cells with ImageJ software of images obtained with a Zeiss LSM700. The cells displayed in Figure 4E were stained with α-GFP (Abcam) after the RRS procedure to visualize the GFP signal.

In Vivo Crosslinking and ChIP-on-Western

The procedure for ChIP in combination with western blot (ChIP-on-Western) has been described previously (Fousteri et al., 2006). Briefly, cells were mock treated or exposed to UV-C light (20 J/m^2) and left to recover for 1 hr at 37°C prior to in vivo crosslinking by 1% formaldehyde at 4°C. Lysis of the crosslinked cells and chromatin purification was performed as described previously (Fousteri et al., 2006). Chromatin shearing was achieved on the Bioruptor Sonicator (Diagenode) using cycles of 30″ ON, 30″ OFF. ChIP was performed on equal amounts of 200–600 bp fragments of chromatin from treated and nontreated cells. Reversal of the crosslinks and elution of the precipitated proteins was performed by extended boiling in Laemmli SDS-sample buffer and analyzed by western blotting (Fousteri et al., 2006).

SUPPLEMENTAL INFORMATION

Supplemental Information includes four figures and Supplemental References and can be found with this article online at http://dx.doi.org/10.1016/j.molcel.2013.08.007.

ACKNOWLEDGMENTS

We would like to thank Florian Lust and Sander Tuit for their assistance, and the Optical Imaging Centre (OIC) of the Erasmus MC for support with microscopes. We thank Niels Galjart for providing the stable GFP-CLIP170-expressing cell line. We also thank Loes van Cuijk for her help testing the activity of the used transcription inhibitors. This work was funded by the Lundbeck Foundation, the Novo Nordisk Foundation, and the Danish Cancer Society (C.D. and J.B.); the European Commission (projects DDResponse and Biomedreg) (J.B.); TOP ALW grant 854.11.002 (H.L.); the Association for International Cancer Research 10-594 (M.T. and W.V.); NSRF 2007–2013, Aristeia-2429, KRHPIS, and ERC-2012-StG-309612 (M.F.); ZonMW TOP grant 912.08.031, Horizon Zenith 93511042, and FP7 Marie Curie International Training Network aDDRess (W.V.); and Erasmus MC fellowship and Dutch Organization for Scientific Research ZonMW Veni Grant 917.96.120 (J.A.M).

Received: May 2, 2013
Revised: June 7, 2013
Accepted: July 17, 2013
Published: August 22, 2013

REFERENCES

Avvakumov, N., Nourani, A., and Côté, J. (2011). Histone chaperones: modulators of chromatin marks. Mol. Cell *41*, 502–514.

Bensaude, O. (2011). Inhibiting eukaryotic transcription: Which compound to choose? How to evaluate its activity? Transcription *2*, 103–108.

Bermejo, R., Lai, M.S., and Foiani, M. (2012). Preventing replication stress to maintain genome stability: resolving conflicts between replication and transcription. Mol. Cell *45*, 710–718.

Birch, J.L., Tan, B.C., Panov, K.I., Panova, T.B., Andersen, J.S., Owen-Hughes, T.A., Russell, J., Lee, S.C., and Zomerdijk, J.C. (2009). FACT facilitates chromatin transcription by RNA polymerases I and III. EMBO J. *28*, 854–865.

Brueckner, F., Hennecke, U., Carell, T., and Cramer, P. (2007). CPD damage recognition by transcribing RNA polymerase II. Science *315*, 859–862.

Carvalho, S., Raposo, A.C., Martins, F.B., Grosso, A.R., Sridhara, S.C., Rino, J., Carmo-Fonseca, M., and de Almeida, S.F. (2013). Histone methyltransferase SETD2 coordinates FACT recruitment with nucleosome dynamics during transcription. Nucleic Acids Res. *41*, 2881–2893.

Cheung, A.C., and Cramer, P. (2011). Structural basis of RNA polymerase II backtracking, arrest and reactivation. Nature *471*, 249–253.

Citterio, E., Van Den Boom, V., Schnitzler, G., Kanaar, R., Bonte, E., Kingston, R.E., Hoeijmakers, J.H., and Vermeulen, W. (2000). ATP-dependent chromatin remodeling by the Cockayne syndrome B DNA repair-transcription-coupling factor. Mol. Cell. Biol. *20*, 7643–7653.

Coin, F., Oksenych, V., Mocquet, V., Groh, S., Blattner, C., and Egly, J.M. (2008). Nucleotide excision repair driven by the dissociation of CAK from TFIIH. Mol. Cell *31*, 9–20.

De Koning, L., Corpet, A., Haber, J.E., and Almouzni, G. (2007). Histone chaperones: an escort network regulating histone traffic. Nat. Struct. Mol. Biol. *14*, 997–1007.

Dinant, C., de Jager, M., Essers, J., van Cappellen, W.A., Kanaar, R., Houtsmuller, A.B., and Vermeulen, W. (2007). Activation of multiple DNA repair pathways by sub-nuclear damage induction methods. J. Cell Sci. *120*, 2731–2740.

Dragestein, K.A., van Cappellen, W.A., van Haren, J., Tsibidis, G.D., Akhmanova, A., Knoch, T.A., Grosveld, F., and Galjart, N. (2008). Dynamic behavior of GFP-CLIP-170 reveals fast protein turnover on microtubule plus ends. J. Cell Biol. *180*, 729–737.

Essers, J., Theil, A.F., Baldeyron, C., van Cappellen, W.A., Houtsmuller, A.B., Kanaar, R., and Vermeulen, W. (2005). Nuclear dynamics of PCNA in DNA replication and repair. Mol. Cell. Biol. *25*, 9350–9359.

Fousteri, M., Vermeulen, W., van Zeeland, A.A., and Mullenders, L.H. (2006). Cockayne syndrome A and B proteins differentially regulate recruitment of chromatin remodeling and repair factors to stalled RNA polymerase II in vivo. Mol. Cell *23*, 471–482.

Gong, F., Kwon, Y., and Smerdon, M.J. (2005). Nucleotide excision repair in chromatin and the right of entry. DNA Repair (Amst.) *4*, 884–896.

Green, C.M., and Almouzni, G. (2003). Local action of the chromatin assembly factor CAF-1 at sites of nucleotide excision repair in vivo. EMBO J. *22*, 5163–5174.

Groisman, R., Polanowska, J., Kuraoka, I., Sawada, J., Saijo, M., Drapkin, R., Kisselev, A.F., Tanaka, K., and Nakatani, Y. (2003). The ubiquitin ligase activity in the DDB2 and CSA complexes is differentially regulated by the COP9 signalosome in response to DNA damage. Cell *113*, 357–367.

Hanawalt, P.C., and Spivak, G. (2008). Transcription-coupled DNA repair: two decades of progress and surprises. Nat. Rev. Mol. Cell Biol. *9*, 958–970.

Heo, K., Kim, H., Choi, S.H., Choi, J., Kim, K., Gu, J., Lieber, M.R., Yang, A.S., and An, W. (2008). FACT-mediated exchange of histone variant H2AX regulated by phosphorylation of H2AX and ADP-ribosylation of Spt16. Mol. Cell *30*, 86–97.

Hoeijmakers, J.H. (2009). DNA damage, aging, and cancer. N. Engl. J. Med. *361*, 1475–1485.

Hondele, M., Stuwe, T., Hassler, M., Halbach, F., Bowman, A., Zhang, E.T., Nijmeijer, B., Kotthoff, C., Rybin, V., Amlacher, S., et al. (2013). Structural basis of histone H2A-H2B recognition by the essential chaperone FACT. Nature *499*, 111–114.

Hoogstraten, D., Nigg, A.L., Heath, H., Mullenders, L.H., van Driel, R., Hoeijmakers, J.H., Vermeulen, W., and Houtsmuller, A.B. (2002). Rapid switching of TFIIH between RNA polymerase I and II transcription and DNA repair in vivo. Mol. Cell *10*, 1163–1174.

Hsieh, F.K., Kulaeva, O.I., Patel, S.S., Dyer, P.N., Luger, K., Reinberg, D., and Studitsky, V.M. (2013). Histone chaperone FACT action during transcription through chromatin by RNA polymerase II. Proc. Natl. Acad. Sci. USA *110*, 7654–7659.

Huang, J.Y., Chen, W.H., Chang, Y.L., Wang, H.T., Chuang, W.T., and Lee, S.C. (2006). Modulation of nucleosome-binding activity of FACT by poly(ADP-ribosyl)ation. Nucleic Acids Res. *34*, 2398–2407.

Kannouche, P.L., Wing, J., and Lehmann, A.R. (2004). Interaction of human DNA polymerase eta with monoubiquitinated PCNA: a possible mechanism for the polymerase switch in response to DNA damage. Mol. Cell *14*, 491–500.

Keller, D.M., and Lu, H. (2002). p53 serine 392 phosphorylation increases after UV through induction of the assembly of the CK2.hSPT16.SSRP1 complex. J. Biol. Chem. *277*, 50206–50213.

Kemble, D.J., Whitby, F.G., Robinson, H., McCullough, L.L., Formosa, T., and Hill, C.P. (2013). Structure of the Spt16 middle domain reveals functional features of the histone chaperone FACT. J. Biol. Chem. *288*, 10188–10194.

Kihara, T., Kano, F., and Murata, M. (2008). Modulation of SRF-dependent gene expression by association of SPT16 with MKL1. Exp. Cell Res. *314*, 629–637.

Kimura, H., and Cook, P.R. (2001). Kinetics of core histones in living human cells: little exchange of H3 and H4 and some rapid exchange of H2B. J. Cell Biol. *153*, 1341–1353.

Krohn, N.M., Stemmer, C., Fojan, P., Grimm, R., and Grasser, K.D. (2003). Protein kinase CK2 phosphorylates the high mobility group domain protein SSRP1, inducing the recognition of UV-damaged DNA. J. Biol. Chem. *278*, 12710–12715.

Lans, H., Marteijn, J.A., and Vermeulen, W. (2012). ATP-dependent chromatin remodeling in the DNA-damage response. Epigenetics Chromatin *5*, 4.

Lejeune, E., Bortfeld, M., White, S.A., Pidoux, A.L., Ekwall, K., Allshire, R.C., and Ladurner, A.G. (2007). The chromatin-remodeling factor FACT contributes to centromeric heterochromatin independently of RNAi. Curr. Biol. *17*, 1219–1224.

Li, Y., Zeng, S.X., Landais, I., and Lu, H. (2007). Human SSRP1 has Spt16-dependent and -independent roles in gene transcription. J. Biol. Chem. *282*, 6936–6945.

Luijsterburg, M.S., Lindh, M., Acs, K., Vrouwe, M.G., Pines, A., van Attikum, H., Mullenders, L.H., and Dantuma, N.P. (2012). DDB2 promotes chromatin decondensation at UV-induced DNA damage. J. Cell Biol. *197*, 267–281.

Marteijn, J.A., Bekker-Jensen, S., Mailand, N., Lans, H., Schwertman, P., Gourdin, A.M., Dantuma, N.P., Lukas, J., and Vermeulen, W. (2009). Nucleotide excision repair-induced H2A ubiquitination is dependent on MDC1 and RNF8 and reveals a universal DNA damage response. J. Cell Biol. *186*, 835–847.

Mayne, L.V., and Lehmann, A.R. (1982). Failure of RNA synthesis to recover after UV irradiation: an early defect in cells from individuals with Cockayne's syndrome and xeroderma pigmentosum. Cancer Res. *42*, 1473–1478.

Menear, K.A., Adcock, C., Boulter, R., Cockcroft, X.L., Copsey, L., Cranston, A., Dillon, K.J., Drzewiecki, J., Garman, S., Gomez, S., et al. (2008). 4-[3-(4-cyclopropanecarbonylpiperazine-1-carbonyl)-4-fluorobenzyl]-2H-phthalazin-1-one: a novel bioavailable inhibitor of poly(ADP-ribose) polymerase-1. J. Med. Chem. *51*, 6581–6591.

Nakazawa, Y., Yamashita, S., Lehmann, A.R., and Ogi, T. (2010). A semi-automated non-radioactive system for measuring recovery of RNA synthesis and unscheduled DNA synthesis using ethynyluracil derivatives. DNA Repair (Amst.) *9*, 506–516.

Nouspikel, T. (2009). DNA repair in mammalian cells : Nucleotide excision repair: variations on versatility. Cell. Mol. Life Sci. *66*, 994–1009.

Pagano, M.A., Meggio, F., Ruzzene, M., Andrzejewska, M., Kazimierczuk, Z., and Pinna, L.A. (2004). 2-Dimethylamino-4,5,6,7-tetrabromo-1H-benzimidazole: a novel powerful and selective inhibitor of protein kinase CK2. Biochem. Biophys. Res. Commun. *321*, 1040–1044.

Polo, S.E., Roche, D., and Almouzni, G. (2006). New histone incorporation marks sites of UV repair in human cells. Cell *127*, 481–493.

Ransom, M., Dennehey, B.K., and Tyler, J.K. (2010). Chaperoning histones during DNA replication and repair. Cell *140*, 183–195.

Reinberg, D., and Sims, R.J., 3rd. (2006). de FACTo nucleosome dynamics. J. Biol. Chem. *281*, 23297–23301.

Schmidt-Zachmann, M.S., Dargemont, C., Kühn, L.C., and Nigg, E.A. (1993). Nuclear export of proteins: the role of nuclear retention. Cell *74*, 493–504.

Schwertman, P., Lagarou, A., Dekkers, D.H., Raams, A., van der Hoek, A.C., Laffeber, C., Hoeijmakers, J.H., Demmers, J.A., Fousteri, M., Vermeulen, W., and Marteijn, J.A. (2012). UV-sensitive syndrome protein UVSSA recruits USP7 to regulate transcription-coupled repair. Nat. Genet. *44*, 598–602.

Smerdon, M.J. (1991). DNA repair and the role of chromatin structure. Curr. Opin. Cell Biol. *3*, 422–428.

Soria, G., Polo, S.E., and Almouzni, G. (2012). Prime, repair, restore: the active role of chromatin in the DNA damage response. Mol. Cell *46*, 722–734.

Stefanini, M., Lagomarsini, P., Giliani, S., Nardo, T., Botta, E., Peserico, A., Kleijer, W.J., Lehmann, A.R., and Sarasin, A. (1993). Genetic heterogeneity of the excision repair defect associated with trichothiodystrophy. Carcinogenesis *14*, 1101–1105.

Stuwe, T., Hothorn, M., Lejeune, E., Rybin, V., Bortfeld, M., Scheffzek, K., and Ladurner, A.G. (2008). The FACT Spt16 "peptidase" domain is a histone H3-H4 binding module. Proc. Natl. Acad. Sci. USA *105*, 8884–8889.

van den Boom, V., Citterio, E., Hoogstraten, D., Zotter, A., Egly, J.M., van Cappellen, W.A., Hoeijmakers, J.H., Houtsmuller, A.B., and Vermeulen, W. (2004). DNA damage stabilizes interaction of CSB with the transcription elongation machinery. J. Cell Biol. *166*, 27–36.

Walmacq, C., Cheung, A.C., Kireeva, M.L., Lubkowska, L., Ye, C., Gotte, D., Strathern, J.N., Carell, T., Cramer, P., and Kashlev, M. (2012). Mechanism of translesion transcription by RNA polymerase II and its role in cellular resistance to DNA damage. Mol. Cell *46*, 18–29.

Winkler, D.D., and Luger, K. (2011). The histone chaperone FACT: structural insights and mechanisms for nucleosome reorganization. J. Biol. Chem. *286*, 18369–18374.

Winkler, D.D., Muthurajan, U.M., Hieb, A.R., and Luger, K. (2011). Histone chaperone FACT coordinates nucleosome interaction through multiple synergistic binding events. J. Biol. Chem. *286*, 41883–41892.

Yarnell, A.T., Oh, S., Reinberg, D., and Lippard, S.J. (2001). Interaction of FACT, SSRP1, and the high mobility group (HMG) domain of SSRP1 with DNA damaged by the anticancer drug cisplatin. J. Biol. Chem. *276*, 25736–25741.

Zlatanova, J., Seebart, C., and Tomschik, M. (2007). Nap1: taking a closer look at a juggler protein of extraordinary skills. FASEB J. *21*, 1294–1310.